THE JOURNAL OF PHYSICAL CHEMISTRY C
A JOURNAL OF THE AMERICAN CHEMICAL SOCIETY

pubs.acs.org/JPCC

Article

Exploring the Effects of Dopamine and DMMP Additives on Improving the Cycle Boosting and Nonflammability of Electrolytes in Full-Cell Lithium-Ion Batteries (18650)

Farshad Boorboor Ajdari,* Abolfazl Fathollahi Zonouz,* Ali Heydari, Hassan Shokoui Mehrabani, Mehdi Shakourian-Fard, Ganesh Kamath, Fatemeh Ghasemi, and Meisam Kahrizi

Cite This: *J. Phys. Chem. C* 2023, 127, 8195−8207

Read Online

ACCESS | Metrics & More | Article Recommendations | Supporting Information

ABSTRACT: Concerns over recyclability, performance, and safety have grown as the use of commercial Li-ion batteries to meet our energy needs has increased. Electrolytes may aid in increased flammability, capacity loss, and safety. Dimethyl methyl phosphonate (DMMP), a flame retardant, and dopamine hydrochloride (DOP) are utilized to increase the cycle life and graphite anode compatibility. The optimal additive formulation (5% wt DMMP and 0.1% wt DOP) reduces inflammability and increases cycle life and reversible capacity (99.14%). Molecular dynamics simulations provide a comprehensive atomistic account of the dynamics of Li^+ ion solvation in the electrolytes and in the presence of additives. Dopamine and DMMP increase the Li-ion solvation-free energy in the electrolyte formulation. While increasing the Li-ion conductivity, additive addition reduces the electrolyte viscosity and enables the formation of a smaller, stronger Li-DMMP-DOP complex than the larger Li-carbonate complex found in Li-neat electrolyte systems. When DMMP and DOP are added to the electrolyte, the carbonates are displaced from the Li-carbonate complex by these additives. The Li-ion solvating nature or compatibility was improved upon the addition of DMMP/DOP further aided by a faster diffusive behavior of the Li complex, which in part would be instrumental in enhancing the performance and safety of the battery electrolyte additive formulations. The modified electrolyte (DMMP 5% wt, DOP 0.1% wt) has a conductivity of 18.60 mS cm^{-1} and a low viscosity at 25 °C. This formulation was evaluated using graphite/NMC-532 cylindrical cells with commercial electrodes. The performance of the graphite/NMC-532 cells containing the modified electrolyte was comparable to those of regular electrolytes based on carbonates: ethylene carbonate/dimethyl carbonate/ethylmethylcarbonate (EC/DMC/EMC) (1:1:1) additions. These findings indicate that DOP and DMMP have a lower oxidation potential (4.3 V) than most commercial electrolytes (4.5 V), preventing cathode deterioration. These insights should pave the path for rational design of practical and cost-effective Li-ion battery electrolyte additive combinations aimed toward lower flammability and improved performance.

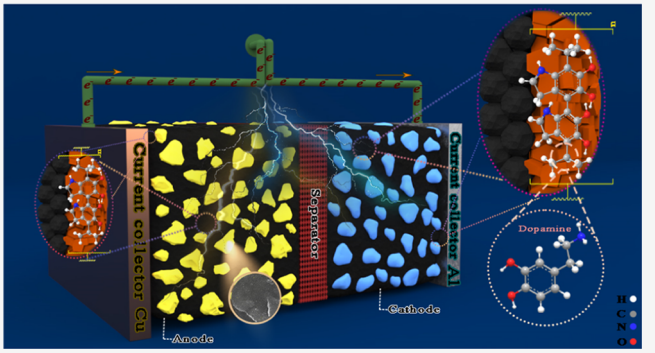

1. INTRODUCTION

Due to fossil fuel depletion and pollution, new energy research focuses on cost-effective and environmentally friendly technology. Lithium-ion batteries have a low self-discharge rate, a longer lifespan, a higher energy density, and a lower price, making them excellent for energy storage in portable electronic devices.[1−6] Safety performance is vital toward this endeavor and has become a technological barrier for industrial production on a broad scale. LIB electrolytes contribute to safety problems with batteries. To reduce the risk of battery fires, researchers have examined safety additives, such as flame retardants and issues relating to overcharging of the batteries.[7−10] Batteries contain flame-retardant chemicals to maintain and protect the electrolytes. They inhibit electrolyte combustion and have a negligible impact on the electrochemical battery performance.[11−14] The generation and dissipation of heat in LIBs is a significant concern.[15−18]

The current thermal effect results in heat generation often caused by the delivery of lithium ions in liquid electrolytes between the anode (graphite) and the cathode (lithium alloy metal oxide). LIBs can disperse heat naturally at slower rates using the thermal effect.[19−21] Impurities such as chlorine, water, and HF significantly affect the performance (eqs 1−4),

Received: November 26, 2022
Revised: April 10, 2023
Published: April 24, 2023

https://doi.org/10.1021/acs.jpcc.2c08293
J. Phys. Chem. C 2023, 127, 8195−8207

dendrite formation, and electrolyte stability, where elevated temperatures mainly produce large amounts of hydrofluoric acid (HF).[22−24] Typically, heat is released from the electrolyte when trace impurities in the water initiate the thermal decomposition of the electrolyte.[25−27]

$$LiPF_6 \leftrightarrow LiF + PF_5 \quad (1)$$

$$PF_5 + H_2O \rightarrow OPF_3 + 2HF \quad (2)$$

$$OPF_{3+2x}Li^+ + 2xe^- \rightarrow LixPF_{3-x}O + xLiF \quad (3)$$

$$OPF_3 + 3H_2O \rightarrow PO_4H_3 + 3HF \quad (4)$$

The instability of the internal components, such as the flammable organic electrolyte, is the immediate cause of thermal runaway issues, resulting in nonflammable, nontoxic, and good interfacial electrode adherence. It inhibits Li dendrite growth, and highly conducting electrolytes can mitigate such risks.[28−32] Internal exothermic processes are the root cause of thermal runaway concerns, which can be classified as (a) faulty operation and releasing oxygen,[33] (b) disintegration of the unstable SEI layer,[34−36] (c) redundant Li plating on the anode, lithium dendrite growth, internal circuit formation, and reactions involving a high amount of heat and gas,[37,38] and (d) oxidation of the carbonate solvent and immediate lithium salt ($LiPF_6$) decomposition.[39−42] The combined effects of all of the chemical reactions can cause LIBs to reach high temperatures and pressures, posing a severe threat of thermal runaway. As a result of the initial analysis, the following practical techniques can be used to prevent LIBs from overheating. It makes the cathode−electrolyte interphase (CEI) film more stable, rendering the electrolyte nonflammable, thereby reducing its flammability.[43−48]

Adding a small amount of flame-retardant chemicals to liquid electrolytes in LIBs reduces their flammability and increases their safety. Flame retardants capture active free radicals from the burning reactions, inhibiting combustion propagation and fires. They function by catalytically eliminating the combustion-generated highly reactive free radicals and blocking these radicals from cascading gas-phase combustion reactions. Halogen retardants, cyclo-phosphazenes, phosphonates, dimethyl(2-methoxy ethoxy)methyl phosphonate (DMMEMP), dimethyl methyl phosphonate (DMMP), composite retardant, and phosphorus additives are the most prevalent flame retardants in LIB electrolytes.[25,49−54] However, they can damage the electrochemical performance, causing failures, ionic conductivity issues, and chemical deterioration. Thus, flame retardant chemical research aims to create nonflammable liquid electrolytes with good electrochemical performance.[55−62]

This study experimentally adjusts the NMC-532-containing full cell with DMMP and dopamine ratios (0.01, 0.05, and 0.1% wt) to obtain simultaneous excellence in flame retardancy and good performance. 5% wt DMMP and 0.1% wt dopamine display the best performance. This approach offers a promising plan to regulate 18650 batteries for various purposes. To provide a comprehensive atomistic picture of the solvation dynamics of Li^+ ions in the electrolyte systems, we perform the potential of mean force calculations and quantify the solvation microstructure around the Li^+ ion. The free energy of solvation of $LiPF_6$ salt in the electrolyte systems is calculated to obtain insight into the solubility of Li^+ ions in the electrolytes. Furthermore, the conductivity and viscosity changes of the electrolyte systems are investigated by calculating the self-diffusion coefficients and are compared with the electrolyte systems' experimentally observed conductivity and viscosity changes.

2. EXPERIMENTAL SECTION

2.1. Materials and Methods. All of the materials used in this work are purchased from Merck Co. They have been used as received and without further treatment.

The electrochemical measurements, including LSV, cyclic voltammetry, and impedance, were conducted by an Autolab Ohm PGSTAT-302N meter.

2.1.1. Preparation. We assembled 5 batteries, one that had no additives (B) and four other batteries consisting of 5% DMMP (D), 5% wt DMMP + 0.01% wt DOP (0.01DP), 5% wt DMMP + 0.05% wt DOP (0.05 DOP), and 5% wt DMMP + 0.1% wt DOP (0.1DP), with B, respectively. In the next step, we weighed the desired values of DOP corresponding to the said ratios. These quantities were separately dissolved in the appropriate electrolyte and were added to the battery. Finally, upon adding DMMP and DOP to the electrolyte, the full-cell cylindrical batteries (18650) were assembled.

2.1.2. Conductivity Test. We investigated the effect of additive concentration on the electrolyte conductivity from the conductivity device. An alternating current (I) was applied across the two electrode plates in the solution to measure the electrical conductivity. A CTR 80 conductivity meter was designed to measure the solutions' electrical conductivity and worked with quadrupole electrodes, unlike conventional conductivity systems.

2.1.3. Viscosity. The most common viscometers currently used are rotary and capillary viscometers. Here, we measured the relative viscosity of electrolytes with an Ostwald micro viscometer.

2.1.4. Self-Extinguishing Time Test System. Due to the importance of safety in the lithium batteries, one of the most critical tests for lithium battery electrolytes is the self-ignition time test (SET). In this test, a flame system and a wick are used. A self-burning time test was performed with different percentages of the additive to investigate the effect of the DMMP additive on commercial liquid electrolytes based on hexafluorophosphate salt.

First, we placed the wick in the electrolyte for a minute to absorb a certain amount of electrolyte. We then ignited it with a flame and recorded the time until the wick was extinguished with a timer. The shorter the burn time relative to the absorbed electrolyte's weight, the more reliable the electrolyte is and therefore can be used as an electrolyte in commercial lithium batteries.

3. RESULTS AND DISCUSSION

The electrolytes on the cathode surface oxidize and decompose during the battery's first charge. We used dopamine hydrochloride (DOP) salt as an electrolyte supplement to overcome this problem. The electrochemical oxidation process forms a layer of polydopamine on the electrolyte, which prevents the electrolyte from oxidizing.[63] The highest occupied molecular orbital (HOMO) and the lowest unoccupied molecular orbital (LUMO) of dopamine and several other organic solvents are reported in ref 63. Dopamine shows the lowest LUMO and highest HOMO among all of these solvents. Dopamine decomposes faster than most other solvents, indicating that

https://doi.org/10.1021/acs.jpcc.2c08293
J. Phys. Chem. C 2023, 127, 8195−8207

Table 1. Values of the Examined Formulations

sample	formulation	additive
B	commercial electrolyte	
D	electrolyte[a] + 5% v DMMP	DMMP
0.01DP	electrolyte + 5% wt DMMP + 0.01% wt DOP	DMMP + DOP
0.05DP	electrolyte + 5% wt DMMP + 0.05% wt DOP	DMMP + DOP
0.1DP	electrolyte + 5% wt DMMP + 0.1% wt DOP	DMMP + DOP

[a]Electrolyte: ethylene carbonate/dimethyl carbonate/ethyl methyl carbonate (EC/DMC/EMC).

it would be the first to decompose. Due to dopamine's greater HOMO and lower LUMO energies, it should theoretically break down before the other electrolyte components and produce a passivation layer or SEI. The LSV data helped researchers comprehend dopamine's oxidative and reductive decomposition (discussed in Section 3.4). According to the computed HOMO energy, the electrolyte containing 5% DMMP and 0.1% wt DOP exhibited a substantially greater oxidative current density than the reference electrolyte. Nevertheless, there are no substantial changes in the reductive current densities.[63,64] It suggested that dopamine would be ineffective as an anode addition. Dopamine may have influenced the electrochemical breakdown of the electrolyte. Therefore, the beneficial effects of dopamine on the cathode in light of the LSV results have drawn us to consider the positive impacts of DOP and DMMP for a safe and high-performance 18650 battery.

The thermal stability of electrolytes with initial percentages and optimal formulation is determined based on the physical and chemical characteristics of the electrolyte system. A performance test was applied to the battery, and samples were electrochemically analyzed. The optimal formulation was then determined and is shown in Table 1.[63]

3.1. Self-Extinguishing Time (SET). It is possible to design nonflammable electrolytes using techniques such as flame-retardant solvents and fluorine-substituted compounds. It is proposed that the flammability characteristics (such as the flash point and combustibility) can be determined using conventional testing. The thermal stability of charged cathodes in contact with very concentrated electrolyte salts should be thoroughly investigated. The production cost of electrolyte synthesis must be decreased, hence encouraging the development of inexpensive, inert, and ecologically safe diluents.[10,65] Phosphorus-containing materials are generally known as flame retardants or antiflammability materials, which react in the vapor phase by a radical mechanism.[66,67] Usually, the amount of phosphorus in these materials can increase the resistance to flammability. Dimethyl methyl phosphonate has a higher content of phosphorus than most other phosphorus-containing substances, such as trimethyl phosphate (TMP),[68] triethyl phosphate (TEP),[69] tributyl phosphate (TBP), and triphenyl phosphate (TPP).[70−72]

In order to investigate the effect of dimethyl methyl phosphonate additive and different amounts of dopamine hydrochloride on commercial liquid electrolytes based on lithium hexafluorophosphate salt ($LiPF_6$), a self-immolation time test was performed. The operations were performed in a glovebox consisting of 99.999% pure inert gas argon to prevent the formation of new electrolyte compounds upon additive inclusion.

The results of the electrolyte flammability test are shown in Figure 1. As can be seen, the commercial-based electrolyte is highly flammable, with a self-ignition time of ∼34 s. By adding

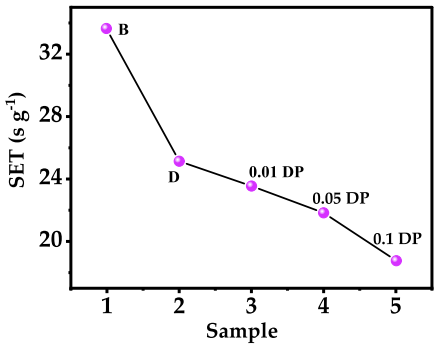

Figure 1. Relationship between the effect of the addition of the additive on the flammability of the lithium battery electrolyte.

5% wt dimethyl methyl phosphonate to the commercial electrolyte, the self-combustion time of the electrolyte is rapidly reduced. Therefore, DMMP was introduced as an additive to reduce the flammability of nonaqueous electrolytes in batteries. Adding dopamine hydrochloride also helps reduce the electrolyte's flammability, as listed in Table S1.

Dimethyl methyl phosphonate in the gaseous state is a suitable radical retainer. This retention of radicals by coupling to hydrogen and hydroxyl radicals in the flame region weakens or even stops the flame chain. Phosphoric acid is also known to decompose and form $PO^{\bullet}$ and $PO_2^{\bullet}$ radicals, which then trap the hydrogen and hydroxyl radicals. In addition, the presence of aromatic rings in dopamine helps to stabilize these radicals and quenches the hydrogen and hydroxyl radicals. The posit reaction for the flame retardation by dimethyl methyl phosphonate in the electrolyte ignition mode is as follows (Scheme 1)[73,74]

As shown in Table S1, the bare electrolyte is highly ignited and remains flammable for a long time. However, the electrolytes containing 0.05% dimethyl methyl phosphonate additive and 0.1% dopamine have a much shorter ignition time and are thus safer (see Figure 2). This article demonstrates the synergistic performance of the DMMP/DOP additives in suppressing and preventing ignition of the structure of the electrolyte in lithium-ion batteries, thus enabling the development of highly flammable and combustible-free secure batteries.

3.2. Conductivity and Viscosity Evaluations. The various formulations of electrolytes were prepared, and their conductivity was measured. The experiment was reproduced four times, and the average from each electrolyte solution was reported. Figure S1a shows the conductivity trend of the different formulated electrolytes, also see Table S2 for tabulated conductivity values. As mentioned, conductivity is an essential factor in determining the electrolyte performance of lithium batteries and is based on the conductivity of the ion in electrolytes. However, many factors, such as salt type,

https://doi.org/10.1021/acs.jpcc.2c08293
J. Phys. Chem. C 2023, 127, 8195−8207

Scheme 1. Possible Mechanism for Dimethyl Methyl Phosphonate Flame-Retardant Additive

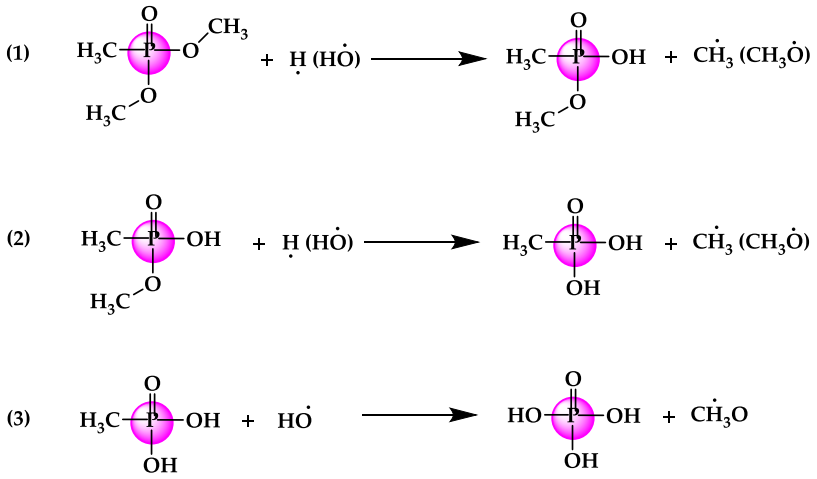

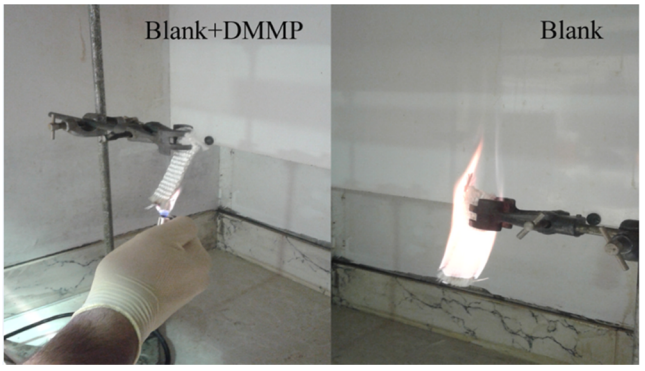

Figure 2. Self-extinguishing time (SET) and ignition test of the bare electrolyte (blank) and resistance of the electrolyte with the additive of dimethyl methyl phosphonate and dopamine against ignition (0.1DP).

solvent, temperature, etc., are responsible for electrolyte conductivity.

The conductivity of the additive-free electrolyte was about 9.56 mS, which dropped to 8.12 mS upon the addition of 5% vol DMMP. However, as the dopamine ratios were increased, the conductivity increased to around 18.60 mS (0.1% wt DOP). While it seems that introducing DMMP to the electrolyte reduces the lithium batteries' performance, adding DMMP enhances thermal stability and prevents electrolyte flammability. The addition of dopamine, on the other hand, improves the battery's safety and promotes its chemical performance.

As the movement of lithium ions inside the electrolyte and between the electrodes is significant, viscosity control is a desired quantity for lithium batteries' performance and conductivity modulation. In a lithium battery electrolyte, conductivity is inversely related to viscosity, so a suitable electrolyte has high conductivity and low viscosity. The DMMP additive has a moderate viscosity among the typical solvents used in lithium batteries. Hence, the resulting electrolyte formulation would still have a suitable viscosity for battery operations. The viscosity of the prepared electrolyte formulations is summarized in Table S3 and shown in Figure S1b.

With an increase in the DMMP content in the electrolytes, the viscosity of the solution also increases, which has particular associated advantages and disadvantages. Due to the increased viscosity of the resulting solution, the compound has a lower vapor pressure at higher temperatures and thus reduces the flammability of the sample. On the other hand, this viscosity increases lithium ions' transfer resistance in the solution. It increases the mass transfer resistance in samples containing additives, thus negatively affecting the battery efficiency. Even with higher percentages of additives, this negative effect is not reduced. Therefore, different amounts of dopamine were used to address the above concern. Dopamine lowers the viscosity of the solution, which, of course, reduces the transfer resistance of lithium ions in the solution.

3.3. Electrochemical Evaluations. To investigate the electrochemical behavior, batteries with lithium nickel cobalt manganese oxide cathode (NMC-532), graphite anode, and 5% DMMP, 5% DMMP + 0.01% wt DOP, 5% DMMP +

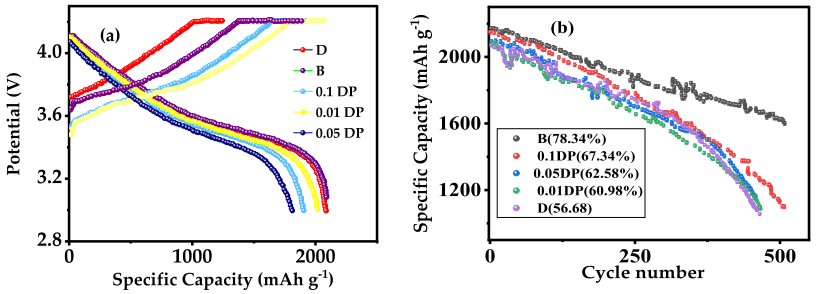

Figure 3. (a) Charging−discharging cycle of the battery and (b) cyclability diagrams for the bare sample and batteries with formulated electrolytes with 5% DMMP and different ratios of dopamine (0.01% wt, 0.05% wt, and 0.1% wt).

https://doi.org/10.1021/acs.jpcc.2c08293
J. Phys. Chem. C 2023, 127, 8195−8207

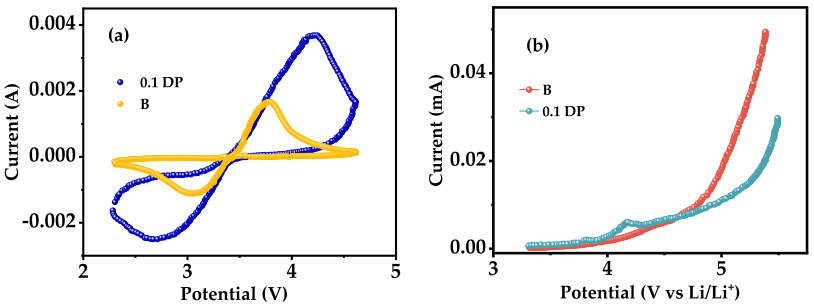

Figure 4. Cyclic voltammetry (a) and LSV (b) plots for the bare sample and DMMP + 0.1% wt DOP-containing sample.

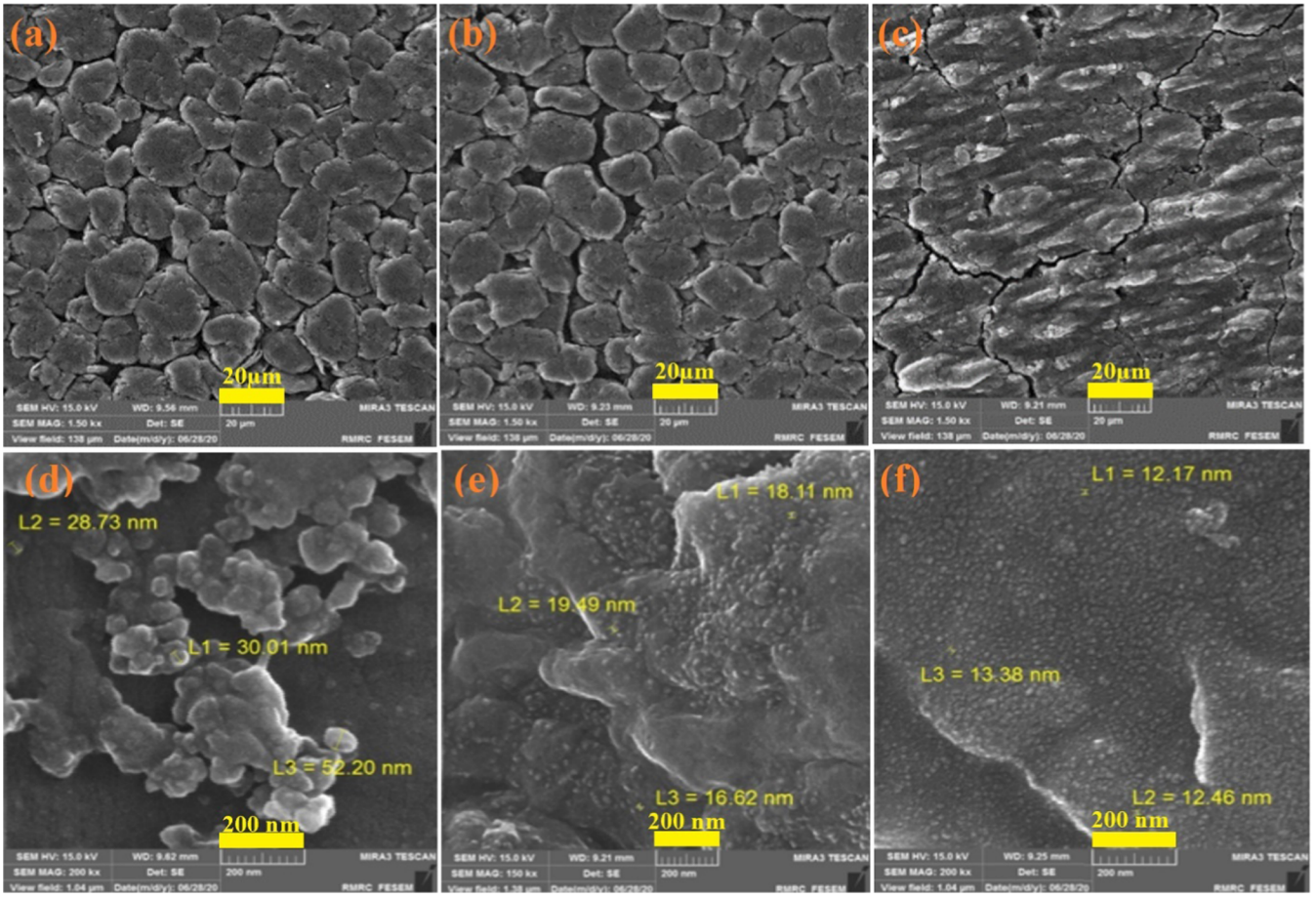

Figure 5. SEM images of the graphite surface for bare (a), 5% wt DMMP (b), and 5% wt DMMP + 0.1DOP (c). SEM images of the cathode surface for bare (d), 5% wt DMMP (e), and 5% wt DMMP + 0.1DOP (f).

0.05% wt DOP, and 5% DMMP + 0.1% wt DOP were fabricated, and their performance was evaluated. As shown in Figure 3a, the sample containing 5% DMMP showed a lower portion of reversible capacity than the commercial electrolyte sample. However, the addition of 0.01% wt dopamine exhibited more satisfying reversibility, and this process was further improved by employing 0.05% wt and 0.1% wt DOP, respectively. The initial discharge also follows the same trend. One can infer that while adding DMMP reduces the initial reversible capacity, small amounts of dopamine improve the capacity. The addition of dopamine compensates for the major drawback of DMMP: a reduction in battery reversibility. The results of the calculations of the initial charge capacity, discharge, and percentage of reversible capacity are listed in Table S4.

Figure 3b shows the cyclicity behavior of the samples with additives and the bare sample after 500 cycles. The details of cyclicity after 300 and 500 cycles are collected in Table S5. The electrolyte containing 5% DMMP has the highest capacity loss, which was to be expected. The vast difference in the capacity drop for 300 and 500 cycles was due to dopamine. The polarization of the lithium ions at the electrode surface and the subsequent consumption of lithium ions in the electrolyte result in the formation of the CEI layer, which subsequently reduces the capacity of the batteries.

Coating organic compounds can improve the CEI formation on the graphite surface and electrochemical reduction of additives, as they have a higher reduction potential than electrolytes. The reduction of the additives in the electrolyte occurs before the electrolyte reduction. It results in an

https://doi.org/10.1021/acs.jpcc.2c08293
J. Phys. Chem. C 2023, 127, 8195−8207

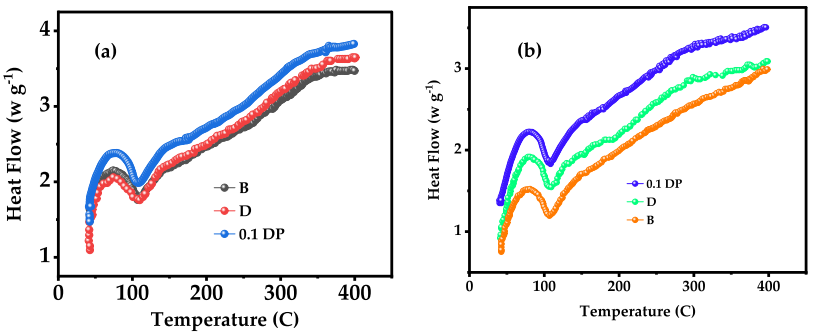

Figure 6. DSC results for graphite (a) and cathode electrodes (b) comparing the effects of DMMP and DOP ratios.

insoluble solid product that contacts the graphite surface and disrupts its catalytic properties. This way, adding additives to the battery reduces gas production and stabilizes the CEI.[75−78]

3.4. LSV and CV Evaluations. The cyclic voltammetry (CV) diagram of the bare electrolyte sample and the sample with the additives is shown in Figure 4a. As seen in the CV plot of the electrolyte with additives, the observed displacement is related to the presence of additives. The addition of DMMP and dopamine to the bare sample makes the peak current higher than in their bare sample counterpart.

In order to investigate the electrochemical stability of the electrolyte, a three-electrode linear scanning voltammetric test of potentials ranging from 3 to 6 V was performed with a scan rate of 0.1 mV. As seen in Figure 4b, the electrolyte containing 5% DMMP + 0.1% dopamine is oxidized at a potential of 4.3 V relative to lithium and tends to be oxidized before the bare electrolyte (4.53). The electrolyte containing 5% DMMP + 0.1% dopamine is oxidized before oxidation and degradation of the solvent. It can thus form a suitable CEI layer on the electrode surface, which is highly consistent with the data obtained from the computational part. The oxidation of dopamine before ethylene carbonate (EC) results in the formation of suitable layers on the electrode surface. In addition, it prevents oxidation and degradation of the ethylene carbonate and an increase in the CEI layer thickness.[72,79]

3.5. Evaluation of Electrode Surface Resistance. The Nyquist diagrams of the electrode charged with the control electrolyte after several charge/discharge cycles are shown in Figure S2. The point of contact with the proper resistance curve at high frequencies represents the ion transfer in the electrolyte called R_s. The following Nyquist chart consists of two semicircles, the first is the film's resistance formed on the electrode surface (RSEI) and the other is the load transfer resistance (R_{ct}). A straight line with a gentle slope can be seen at low frequencies, indicating the electrode's mass transfer.

As can also be seen, the values related to the solution strength of both the samples are almost the same. The factors relating to the charge transfer resistance at the electrode surface are virtually identical. However, with a slight difference, the charge transfer resistance at the electrode surface consisting of the bare electrolyte is lowered. The difference in the slope of the Warburg resistance line indicates the facilitation of the passage of lithium ions into the electrode structure. The slope of the Warburg line is higher in samples containing 5% DMMP + 0.1% dopamine, facilitating the passage of lithium ions. It supports the observed electrochemical and cyclic behavior of the electrolyte. However, we note that the amount of Warburg impedance depends on the morphology and thickness of the electrode surface.[80]

3.6. Structural Examination of the Electrode Surface. The scanning electron microscopy (SEM) technique was used to evaluate batteries' particle size and morphology in the presence and absence of additives (SEM, JEOL JSM-7001F/SHL, JEOL Inc.). After performing the electrochemical operation, the batteries were opened and washed with EMC to remove the residual electrolytes on the anode or cathode and kept in a vacuum chamber for 12 h.

Morphological studies of the graphite electrode and the NMC-532 electrode surface for the bare, 5% wt DMMP, and 5% wt DMMP + 0.1% wt DOP samples were conducted, and the results of the 0th cycle and 500th cycle are shown in Figure 5. The surface of the graphite electrode containing 5% DMMP + 0.1% wt DOP (see Figure 5c) is much healthier and more uniform than the surfaces consisting of 5% wt DMMP (Figure 5b) and bare samples (Figure 5a), respectively.

These figures suggest that the graphitic surface of the bare sample (Figure 5a) is degraded due to the decomposition of the electrolyte and $LiPF_6$ salt. The degradation rate is much lower for the electrolyte consisting of 5% DMMP (Figure 5b) and 5% wt DMMP + 0.1% wt DOP (Figure 5c) samples, thereby strengthening the electrochemical data. The surface of NMC-532 with 5% wt DMMP (Figure 5f) + 0.1% DOP is much healthier than the 5% wt DMMP (Figure 5e) or the surface with the bare samples (Figure 5d).

A look at the cathode suggested that with a 5% wt DMMP + 0.1% wt DOP, a uniformly coated layer is present on the surface, facilitating successful Li^+ insertion/de-insertion. Lithium fluoride (LiF) is an insulating compound against electrons and lithium ions. The dissolution of lithium fluoride and the formation of polycarbonate ($R\text{-}CH_2OCO_2\text{-}Li$) on the electrode surface facilitate the transfer of lithium ions to the electrode.[80] Phosphorus-based additives also dissolve the lithium fluoride formed during the oxidation state on the cathode surface and prevent the electrode surface from decomposing, consistent with the previous observations.[66] In addition, the particle size (0.1DP < D < B) indicates that the addition of additives helps in reducing the particle size and increases the efficiency of the batteries (Figure 5d−f).

The X-ray diffraction (XRD) technique was used to investigate the changes in the crystallinity of the batteries in the presence and absence of 5% DMMP and 5% DMMP + 0.1% dopamine. As shown in Figure S3, a peak severity decrease occurred upon adding dopamine. This decreasing trend observed in the XRD analysis (R_{int}-2000, Rigaku, Cu/Kα radiation, 2θ = 10−90°) could be due to the decomposition/amorphization of the dopamine within the electrolyte. Reducing the crystallinity could decrease the resistance and increase the charge and discharge of the sample. The 5% wt

https://doi.org/10.1021/acs.jpcc.2c08293
J. Phys. Chem. C 2023, 127, 8195−8207

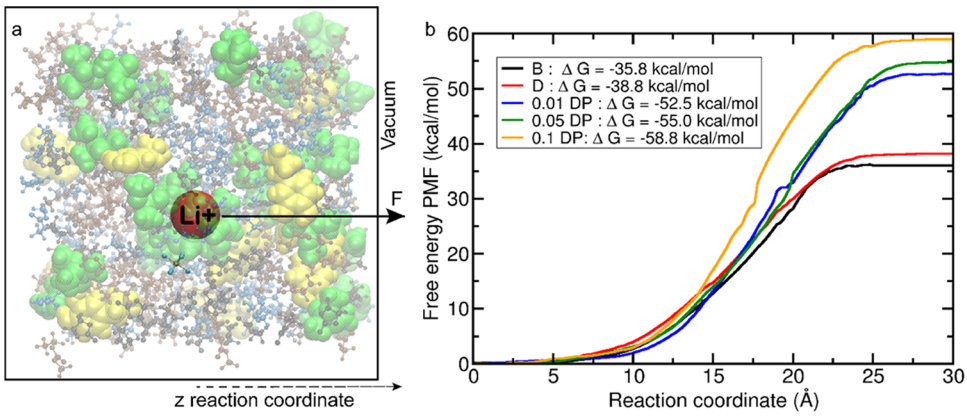

Figure 7. Free energy of solvation profiles generated with ABF-MD for Li^+ ion solvation transferred from five different electrolyte phases to vacuum. (a) Li ion, shown as a red sphere, is subject to a force F in the z direction corresponding to the reaction coordinate. The PF_6 anion is shown as CPK representation along with EC, DMC, and EMC. The yellow van der Waals spheres are dopamine, and the green spheres are DMMP, respectively. Six windows of 5 Å width each are used to compute the potential of mean force. The free energy is computed as the difference in the free energy of the lithium ion in a vacuum to the free energy value of the lithium cation in the electrolyte-rich phase. The potential of mean force profiles for the lithium cation in various electrolytes and electrolytes + additives (B, D, 0.01DP, 0.05DP, and 0.1DP) are shown on the right. Reaction coordinate z = 0 Å indicates that the lithium cation is present in the electrolyte/electrolyte + additives' rich phase, and z = 20−30 Å suggests that the lithium cation is in a vacuum. The larger the free energy of the solvation of lithium in the solvent, the greater is the affinity of the lithium cation in the electrolyte/(electrolyte + additives) phase. (b) We show the PMF profiles across the reaction coordinate z, where the force F is applied on the lithium cation. One sees that as we increase the dopamine additive in the electrolyte with DMMP, the lithium likes the electrolyte phase having a more negative free energy (−55 and −58.8 kcal/mol for 0.05DP and 0.1DP, respectively). Adding DMMP and dopamine to the electrolytes results in increased affinity for the lithium cation when compared to a scenario with no additives (for B and D, the lithium solvation is much lower (−35.8 and −38.8 kcal/mol, respectively)).

DMMP sample showed an increase in the intensity of the peaks, indicating a rise in the crystallinity of the cathodic material.

The samples' peaks for 5%wt DMMP + 0.1%wt DOP were slightly displaced compared to the bare and 5% wt DMMP samples, indicating the formation of a layer resulting from the decomposition of the cathodic material. X-ray studies show that the presence of dopamine additive improves electrochemical performance by forming a layer on the cathode surface, which is entirely consistent with the results of electron microscopy images and cyclicity.[81−83] Figure 6 shows the DSC test curve for bare, 5% wt DMMP, and 5% wt DMMP + 0.1% DOP samples. According to the results, the structure pattern of all three samples is similar; however, as observed in the SET test section, the 5% wt DMMP + 0.1% wt DOP sample appeared at higher temperatures than other samples. It has been shown that additives increase the thermal stability of the electrolyte. Additives increase the heat capacity of the electrolyte and, as a result, increase the degradation temperature and transfer the corresponding peak to higher temperatures. They further diminish the heat produced by the oxidation of the sample.

The NMC-532 cathodes were tested after 500 cycles of charging and discharging for bare and additive-containing samples. As shown in Figure 6b, the bare cathode starts to deteriorate at a lower temperature than the sample with 5% wt DMMP + 0.1% wt DOP and has a lower thermal stability. At the same time, the 5% DMMP + 0.1% dopamine sample has higher thermal stability than the bare electrode due to the formation of a layer on the electrode surface (the oxidation layer of DMMP improves the thermal stability of the electrode).[82,84]

During overcharging, oxidation of the cathode material results in gases, such as oxygen, which combust and explode. The closed environment and the decomposition of the electrode cause a sudden increase in temperature and lead to heat escape and the eventual explosion of the cell. Despite the layer formed on the electrode surface, the electrode's thermal stability increases, thus preventing premature electrode destruction and battery outbreak. Therefore, DMMP and DOP additives prevent the electrode's explosion and collapse, prevent the electrolyte from igniting during a fire, ignite the battery, and suppress the flame.

We performed two sets of measurements and calculations of each sample to ensure the reproducibility of our findings (see Figure S4). The results of both batteries were very close to one another (Table S6), confirming the data's repeatability and highlighting its accuracy.

4. COMPUTATIONAL DETAILS

The adaptive bias force (ABF) method[85] is suitable for accurately predicting the free energy of solvation, hydration, partition coefficients of various organic compounds,[86,87] and exfoliation and stabilization energetic nanomaterials in different solvents, such as ionic liquids.[87] Recently, this method has been used to predict the free energy of solvation of Li^+,[88] Na^+,[89] and Mg^{2+}[90] ions in different cyclic and acyclic nonaqueous carbonates and their binary mixtures with application in ion batteries. In this study, we applied the ABF method[85] adopted in NAMD version 2.7b3[91] to predict the free energy of solvation of Li^+ ions in the B (commercial electrolyte), D (electrolyte + 5% v DMMP), 0.01DP (electrolyte + 5% v DMMP + 0.01% wt DOP), 0.05DP (electrolyte + 5% v DMMP + 0.05% wt DOP), and 0.1DP (electrolyte + 5% v DMMP + 0.1% wt DOP) electrolytes. An all-atom force field based on the CHARMM General Force field (CGENFF)[92] was used in this work to model the B, D, 0.01DP, 0.05DP, and 0.1DP electrolytes and the salt interactions. In the ABF method, the Li^+ ion in the complex with the PF_6^- anion is solvated in the electrolytes of B, D,

https://doi.org/10.1021/acs.jpcc.2c08293
J. Phys. Chem. C 2023, 127, 8195−8207

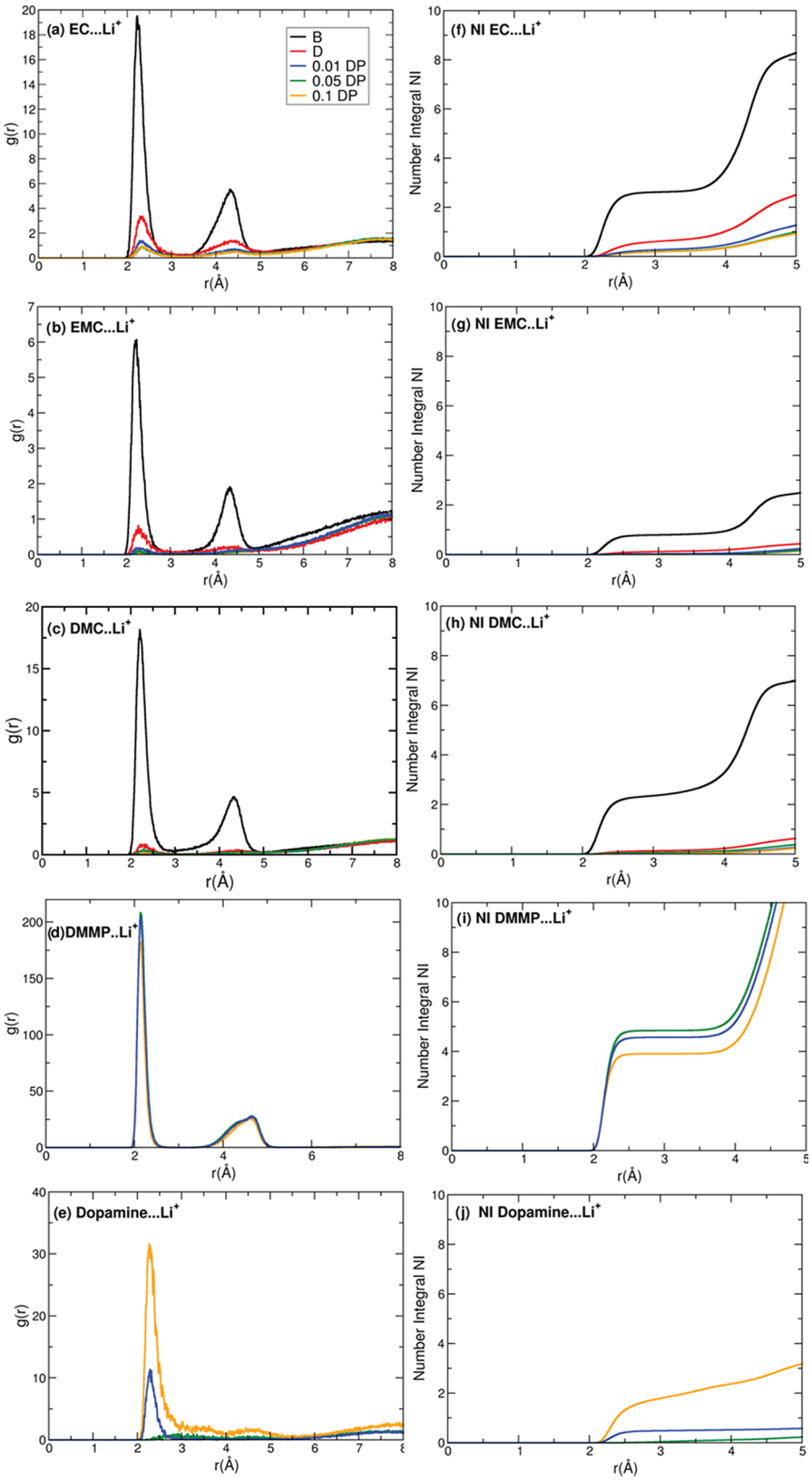

Figure 8. Radial distribution function (RDF) and number integral for Li^+ ion interaction with the electrolytes. For B (EC/EMC/DMC), the interactions of EC, EMC, and DMC carbonyl oxygen interactions with the Li cation are shown in black (a–c). The carbonyl oxygen of the carbonates interacts favorably with the lithium cation. For electrolyte D (EC/EMC/DMC with 5% DMMP), the interactions of carbonyl oxygen of EC/EMC/DMC and phosphate oxygen of DMMP with the lithium cation is shown in red (a–d). For electrolytes 0.01DP, 0.05DP, and 0.1DP, there are five chemicals, namely, ethylene carbonate (EC), ethyl methyl carbonate (EMC), dimethyl carbonate (DMC), dimethyl methyl phosphate (DMMP), and dopamine. The interaction of amide-nitrogen in dopamine with the lithium cation in 0.01DP, 0.05DP, and 0.1DP (e). The corresponding number integral is obtained by integrating the $g(r)$ (f–j).

https://doi.org/10.1021/acs.jpcc.2c08293
J. Phys. Chem. C 2023, 127, 8195–8207

0.01DP, 0.05DP, and 0.1DP. The Li^+ ion is subjected to a force F and moved from the electrolyte-rich phase to the vacuum. The free energy of solvation is based on the integration of the applied force F along the reaction coordinate (z) and is computed based on the free energy difference in the electrolyte-rich phase and vacuum. We follow a similar protocol, and the simulation details are discussed at length in the works of Shakourian-Fard et al. and Kamath et al.[88−90] Further computational details, including force field parameters, and sample inputs are provided in the Supporting Information and attachments. The free energy as obtained from the potential of mean force calculations and associated equations can be found in the works of Darve and Pohorille.[85] Some of these equations are also provided in the Supporting Information.

The free energy of solvation of Li^+ ions in the electrolytes can be computed by the potential of mean force (PMF) simulations. The computed free energy profiles of Li^+ ions with the PF_6^- anion in the B, D, 0.01DP, 0.05DP, and 0.1DP electrolytes as a distance function along the reaction coordinate are shown in Figure 7. The Gibbs free energy PMF (ΔG) is the free energy change that transfers a Li^+ ion from the vacuum to the condensed phase. The ΔG values were computed based on the difference in the free energy of the first window (Li^+ ion in the electrolyte-rich phase) and the last window (Li^+ ion in the vacuum phase). The ΔG values are used to understand the solubility and solvation characteristics of the Li^+ ion in the electrolytes. The ΔG values for the Li^+ ion in the B, D, 0.01DP, 0.05DP, and 0.1DP electrolytes are presented in Figure 7. The higher the ΔG value, the greater the solubility of the Li^+ ion in that electrolyte. The rank order for the solubility of Li^+ ion in the B, D, 0.01DP, 0.05DP, and 0.1DP electrolytes is in the range of −35.8 to −58.8 kcal/mol and follows the order 0.1DP > 0.05DP > 0.01DP > D > B. This order shows that the solubility of Li^+ ions increases by adding the D and DP additives to the B electrolyte. Furthermore, an increase in the concentration of DP additive from 0.05% wt to 0.1% wt enhances the solubility of the Li^+ ion in the electrolyte.

In order to provide an atomistic picture of the differences in the solubility of Li^+ ions in the electrolytes, the interactions between the Li^+ ion and the electrolytes are analyzed. The Li^+ coordination with the atoms of the electrolytes in the first solvation shell shows the solvation behavior of the Li^+ ion in the electrolytes.

We compute the pairwise radial distribution functions (RDFs) for the Li^+ ion interaction with the various polar atoms on the electrolytes and their additives. Our earlier studies[85−87] found that the Li^+ ion forms a strong complex with the carbonyl oxygen of EC, EMCA, and DMCA. It is evident from the first peak around 2.4 Å as seen in Figure 8a−c for Li^+ in the electrolyte mixture without additives (B). As previously demonstrated, the interaction of the Li^+ ion with carbonyl oxygen is more dominant than the interaction with ethereal oxygen in carbonates. With the addition of DMMP, the interaction of Li^+ with the carbonates is reduced, and the phosphate oxygen starts to form stronger interactions with Li^+ and displaces the carbonates from the complex. It is evident from the reduction of the first peak for the carbonate oxygen with Li^+ (system D) and the sharp rise observed for DMMP interaction with the Li^+ ion (see Figure 8d). With the addition of dopamine to the electrolytes and DMMP, we now see an increasing interaction of the amide-nitrogen atom in dopamine with Li^+, and at 0.1% wt (0.1DP), the interaction of dopamine with Li^+ is very strong, suggesting that dopamine also competes with DMMP to form a complex with the Li^+ ion, see Figure 8e. The corresponding number integrals (see Figure 8f−j) are also provided, confirming the presented RDFs. A fewer number (1−2 DMMP and 1−2 dopamine molecules (depending on the ratio)) binds with the Li, preventing the carbonates (normally 4−6 carbonates bind to the Li) from accessing the Li and hence resulting in a smaller Li-based DMMP and DOP complex. This complex is able to diffuse faster in the less viscous electrolyte additive system. The smaller size yet stronger Li-DMMP-DOP complex compared to the Li-carbonate complex is responsible for higher free energy of solvation of Li in the presence of DOP and DMMP and increased diffusion.

We also computed the self-diffusion coefficient (D) of the Li^+ ion in the electrolytes using the Einstein relation as follows (eq 5)

$$D = \frac{1}{6}\lim_{t\to\infty}\frac{\mathrm{d}(\mathrm{MSD})}{\mathrm{d}(t)} \tag{5}$$

The diffusion coefficient is computed as the slope of the mean square displacement (MSD) of the cation/anion versus time (t) simulation time scale. Additional details and plots of MSD as a function of time can be seen in the Supporting Information (Figure S5 and Table S7).

The computed self-diffusion coefficient values of the Li^+ ion in the B, D, 0.01DP, 0.05DP, and 0.1DP electrolytes are shown in Figure 9. As seen in Figure 9, adding the D and DP additives

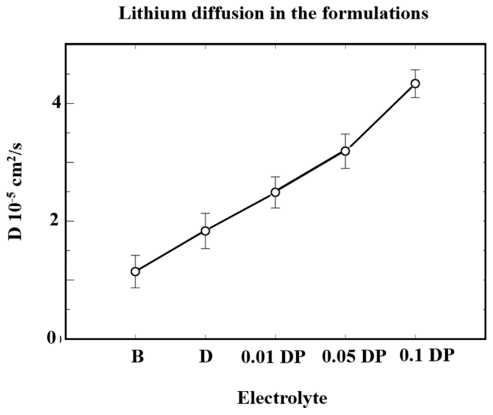

Figure 9. Computed self-diffusion coefficient values of Li^+ ions in the B, D, 0.01DP, 0.05DP, and 0.1DP electrolytes.

increases the self-diffusion coefficient value of the Li^+ ion in the B electrolyte. Hence, the Li^+ ion can move more freely, and thus, the conductivity increases. On the other hand, the self-diffusion coefficient value for the Li^+ ion in the DP electrolyte increases with an increase in the concentration of DP additive from 0.05% wt to 0.1% wt. It should be mentioned that the self-diffusion coefficients determined from molecular dynamics simulations are generally consistent with the experimentally observed conductivity and viscosity changes of the electrolyte systems. The higher the self-diffusion coefficients, the higher the conductivity and diffusive ability of the Li^+ ion in the electrolyte system, and the lower the viscosity. The addition of DMMP and dopamine results in the reduction of viscosity as well as the formation of the DMMP/dopamine-Li complex, which dominates over the carbonate-Li complex. The increased diffusion of Li with the addition of DMMP and

https://doi.org/10.1021/acs.jpcc.2c08293
J. Phys. Chem. C 2023, 127, 8195−8207

DOP may be partly responsible for the improved conductivity and performance of the cells.

5. CONCLUSIONS

Better safety standards are critical and imperative for lithium-ion batteries as they become synonymous with next-generation green energy alternatives. For lithium-ion batteries, reducing electrolyte flammability is considered a promising way to increase the safety of lithium batteries. It can be achieved by adding antiflammable additives such as dimethyl methyl phosphonate. However, a significant concern with these materials is the reduced chemical performance of the battery. Therefore, we simultaneously use dimethyl methyl phosphonate and dopamine hydrochloride in 18650 batteries to increase the thermal stability and reduce the electrolyte's flammability while taking a minor hit on the electrochemical performance of the battery. The PMF-free energy calculations reveal that the rank order for the solubility of the Li^+ ion in the B, D, 0.01DP, 0.05DP, and 0.1DP electrolytes follows the order 0.1DP > 0.05DP > 0.01DP > D > B. This order shows that the solubility of the Li^+ ion increases by adding the D and DP additives to the B electrolyte and by increasing the concentration of the DP additive from 0.05% wt to 0.1% wt. This increased solvation of Li with DMMP and DOP is coupled with the formation of smaller complexes that can diffuse faster through the lesser viscous electrolyte formulation, resulting in increased conductivity and partly responsible for improved Li-ion performance.

These computational results agree with the electrolyte systems' experimentally observed conductivity and viscosity changes. Our results show that the 5% wt DMMP + 0.1% wt DOP addition to the bare electrolyte significantly increased safety and substantially improved the electrochemical performance over a 300 complete charge−discharge cycle set. Further, the temperature stability was nearly twice as high as its bare electrolyte counterpart. However, only a 3% capacity drop was observed for 0.1% DP compared to the bare sample.

We have demonstrated that adding DOP and DMMP to bare electrolytes provides a cost-effective solution for improved battery performance and safety. Some salient features include the solid state of DMMP and DOP, which are easy to work with and do not require special processing. Second, these additives are easily dissolved in electrolytes. Finally, DMMP also eliminates the acid (HF) formation as one gets with the bare electrolyte. This should pave the path for rational design and engineering novel electrolyte additive formulations for increased battery safety and performance.

ASSOCIATED CONTENT

Supporting Information

The Supporting Information is available free of charge at https://pubs.acs.org/doi/10.1021/acs.jpcc.2c08293.

Conductivity/viscosity as a function of additive formulation; Nyquist plots; XRD plots; reproducibility of reported values; further description of the potential of mean force calculations including computational results; and diffusion calculations/plots (PDF)

Additional force field parameters (ZIP)

AUTHOR INFORMATION

Corresponding Authors

Farshad Boorboor Ajdari − *Department of Applied Chemistry, Faculty of Chemistry, University of Kashan, Kashan 87317-53153, Iran*; orcid.org/0000-0002-8660-0474; Email: f.boorboor@kashanu.ac.ir, farshadborbor.2009@gmail.com

Abolfazl Fathollahi Zonouz − *Department of Chemistry, University of Isfahan, Isfahan 81746-73441, Iran*; Email: zonoziabf@gmail.com

Authors

Ali Heydari − *Department of Chemistry, University of Sistan and Baluchestan, Zahedan 98155-987, Iran*

Hassan Shokoui Mehrabani − *Faculty of Mechanical Engineering, Iran University of Science and Technology (IUST), Tehran 16846-13114, Iran*

Mehdi Shakourian-Fard − *Department of Chemical Engineering, Birjand University of Technology, Birjand 97198-66981, Iran*; orcid.org/0000-0002-5454-3698

Ganesh Kamath − *Dalzierfiver LLC, El Sobrante, California 94803, United States*; orcid.org/0000-0002-6957-1173

Fatemeh Ghasemi − *Department of Applied Chemistry, Faculty of Chemistry, University of Kashan, Kashan 87317-53153, Iran*

Meisam Kahrizi − *Research Laboratory of Real Samples Analysis, Faculty of Chemistry, Iran University of Science and Technology (IUST), Tehran 16846-13114, Iran*

Complete contact information is available at: https://pubs.acs.org/10.1021/acs.jpcc.2c08293

Notes

The authors declare no competing financial interest.

ACKNOWLEDGMENTS

The authors gratefully acknowledge financial support from the University of Kashan and the Research Council of Birjand University of Technology.

REFERENCES

(1) Jiang, Z. Y.; Li, H. B.; Qu, Z. G.; Zhang, J. F. Recent Progress in Lithium-Ion Battery Thermal Management for a Wide Range of Temperature and Abuse Conditions. *Int. J. Hydrogen Energy* **2022**, *47*, 9428−9459.

(2) Bicy, K.; Gueye, A. B.; Rouxel, D.; Kalarikkal, N.; Thomas, S. Lithium-Ion Battery Separators Based on Electrospun PVDF: A Review. *Surf. Interfaces* **2022**, *31*, No. 101977.

(3) Ghany, N. A. A.; Elsherif, S. A.; Handal, H. T. Revolution of Graphene for Different Applications: State-of-the-Art. *Surf. Interfaces* **2017**, *9*, 93−106.

(4) Lin, Z.; Lan, X.; Xiong, X.; Hu, R. Recent Development of Sn−Fe-Based Materials as a Substitute for Sn−Co−C Anodes in Li-Ion Batteries: A Review. *Mater. Chem. Front.* **2021**, *5*, 1185−1204.

(5) Nitta, N.; Wu, F.; Lee, J. T.; Yushin, G. Li-Ion Battery Materials: Present and Future. *Mater. Today* **2015**, *18*, 252−264.

(6) Zhang, X.; Huang, X.; Liu, D.; Hoang, T. K. A.; Geng, X.; Chen, P.; Zhang, X.; Wen, G. Binderless, Bendable Graphene/FexSn1-XO2 Anode for Lithium-Ion Batteries without the Necessity of a Current Collector. *Int. J. Hydrogen Energy* **2018**, *43*, 21428−21440.

(7) Wen, J.; Yu, Y.; Chen, C. A Review on Lithium-Ion Batteries Safety Issues: Existing Problems and Possible Solutions. *Mater. Express* **2012**, *2*, 197−212.

(8) Bicy, K.; Mathew, D. E.; Stephen, A. M.; Royaud, I.; Poncot, M.; Godard, O.; Aranda, L.; Rouxel, D.; Kalarikkal, N.; Thomas, S. Sustainable Lithium-Ion Battery Separators Derived from Poly-

ethylene Oxide/Lignocellulose Coated Electrospun P(VDF-TrFE) Nanofibrous Membranes. *Surf. Interfaces* **2022**, *29*, No. 101716.
(9) Wan, S.; Chen, S. A Dithiol-Based New Electrolyte Additive for Improving Electrochemical Performance of NCM811 Lithium Ion Batteries. *Ionics* **2020**, *26*, 6023−6033.
(10) Zhang, S.; Li, S.; Lu, Y. Designing Safer Lithium-Based Batteries with Nonflammable Electrolytes: A Review. *eScience* **2021**, *1*, 163−177.
(11) Chen, M.; Mei, J.; Wang, S.; Chen, Q.; Zhao, L.; Kong, Q.; Wu, X. Comparative Studies on the Combustion Characters of the Lithium-Ion Battery Electrolytes with Composite Flame-Retardant Additives. *J. Energy Storage* **2022**, *47*, No. 103642.
(12) Li, H.; Kuai, Y.; Yang, J.; Hirano, S.; Nuli, Y.; Wang, J. A New Flame-Retardant Polymer Electrolyte with Enhanced Li-Ion Conductivity for Safe Lithium-Sulfur Batteries. *J. Energy Chem.* **2022**, *65*, 616−622.
(13) Gibertini, E.; Carosio, F.; Aykanat, K.; Accogli, A.; Panzeri, G.; Magagnin, L. Silica-Encapsulated Red Phosphorus for Flame Retardant Treatment on Textile. *Surf. Interfaces* **2021**, *25*, No. 101252.
(14) Baddam, Y.; Ijaola, A. O.; Asmatulu, E. Fabrication of Flame-Retardant and Superhydrophobic Electrospun Nanofibers. *Surf. Interfaces* **2021**, *23*, No. 101017.
(15) Liu, Y.; Yao, M.; Zhang, L.; Niu, Z. Large-Scale Fabrication of Reduced Graphene Oxide-Sulfur Composite Films for Flexible Lithium-Sulfur Batteries. *J. Energy Chem.* **2019**, *38*, 199−206.
(16) Han, C.; Xing, W.; Zhou, K.; Lu, Y.; Zhang, H.; Nie, Z.; Xu, F.; Sun, Z.; Du, Y.; Yu, H.; Li, R.; Zhu, J. Self-Assembly of Two-Dimensional Supramolecular as Flame-Retardant Electrode for Lithium-Ion Battery. *Chem. Eng. J.* **2022**, *430*, No. 132873.
(17) Mei, N.; Xu, X.; Li, R. Heat Dissipation Analysis on the Liquid Cooling System Coupled with a Flat Heat Pipe of a Lithium-Ion Battery. *ACS Omega* **2020**, *5*, 17431−17441.
(18) Li, H.; Zhang, B.; Liu, W.; Lin, B.; Ou, Q.; Wang, H.; Fang, M.; Liu, D.; Neelakandan, S.; Wang, L. Effects of an Electrospun Fluorinated Poly(Ether Ether Ketone) Separator on the Enhanced Safety and Electrochemical Properties of Lithium Ion Batteries. *Electrochim. Acta* **2018**, *290*, 150−164.
(19) Xia, L.; Wang, D.; Yang, H.; Cao, Y.; Ai, X. An Electrolyte Additive for Thermal Shutdown Protection of Li-Ion Batteries. *Electrochem. Commun.* **2012**, *25*, 98−100.
(20) Wu, W.; Wang, S.; Wu, W.; Chen, K.; Hong, S.; Lai, Y. A Critical Review of Battery Thermal Performance and Liquid Based Battery Thermal Management. *Energy Convers. Manage.* **2019**, *182*, 262−281.
(21) Ishikawa, M.; Machino, S.; Morita, M. Electrochemical Control of a Li Metal Anode Interface: Improvement of Li Cyclability by Inorganic Additives Compatible with Electrolytes. *J. Electroanal. Chem.* **1999**, *473*, 279−284.
(22) Zhang, S. S. A Review on Electrolyte Additives for Lithium-Ion Batteries. *J. Power Sources* **2006**, *162*, 1379−1394.
(23) Wu, B.; Pei, F.; Wu, Y.; Mao, R.; Ai, X.; Yang, H.; Cao, Y. An Electrochemically Compatible and Flame-Retardant Electrolyte Additive for Safe Lithium Ion Batteries. *J. Power Sources* **2013**, *227*, 106−110.
(24) Heine, J.; Hilbig, P.; Qi, X.; Niehoff, P.; Winter, M.; Bieker, P. Fluoroethylene Carbonate as Electrolyte Additive in Tetraethylene Glycol Dimethyl Ether Based Electrolytes for Application in Lithium Ion and Lithium Metal Batteries. *J. Electrochem. Soc.* **2015**, *162*, A1094.
(25) Zonouz, A. F. Investigation the Effect of DMMP as Electrolyte Additive on the Flammability and Electrochemical Properties of Lithium-Ion Batteries. *Anal. Bioanal. Electrochem.* **2018**, *10*, 1053−1063.
(26) Han, Y.-K.; Yoo, J.; Yim, T. Distinct Reaction Characteristics of Electrolyte Additives for High-Voltage Lithium-Ion Batteries: Tris (Trimethylsilyl) Phosphite, Borate, and Phosphate. *Electrochim. Acta* **2016**, *215*, 455−465.
(27) Han, Y.-K.; Yoo, J.; Yim, T. Why Is Tris (Trimethylsilyl) Phosphite Effective as an Additive for High-Voltage Lithium-Ion Batteries? *J. Mater. Chem. A* **2015**, *3*, 10900−10909.
(28) Wang, Q.; Jiang, L.; Yu, Y.; Sun, J. Progress of Enhancing the Safety of Lithium Ion Battery from the Electrolyte Aspect. *Nano Energy* **2019**, *55*, 93−114.
(29) Zheng, Q.; Xing, L.; Yang, X.; Li, X.; Ye, C.; Wang, K.; Huang, Q.; Li, W. N-Allyl-N,N-Bis(Trimethylsilyl)Amine as a Novel Electrolyte Additive To Enhance the Interfacial Stability of a Ni-Rich Electrode for Lithium-Ion Batteries. *ACS Appl. Mater. Interfaces* **2018**, *10*, 16843−16851.
(30) Li, X.; Guo, L.; Li, J.; Wang, E.; Liu, T.; Wang, G.; Sun, K.; Liu, C.; Peng, Z. Reversible Cycling of Graphite Electrodes in Propylene Carbonate Electrolytes Enabled by Ethyl Isothiocyanate. *ACS Appl. Mater. Interfaces* **2021**, *13*, 26023−26033.
(31) Sawayama, S.; Ochi, R.; Mimura, H.; Morita, M.; Fujii, K. 2,2,2-Trifluoroethyl Acetate as an Electrolyte Solvent for Lithium-Ion Batteries: Effect of Weak Solvation on Electrochemical and Structural Characteristics. *J. Phys. Chem. C* **2021**, *125*, 27098−27105.
(32) Li, R.; Zhao, P.; Qin, X.; Li, H.; Qu, K.; Jiang, D. First-Principles Study of Heterostructures of MXene and Nitrogen-Doped Graphene as Anode Materials for Li-Ion Batteries. *Surf. Interfaces* **2020**, *21*, No. 100788.
(33) Mu, L.; Lin, R.; Xu, R.; Han, L.; Xia, S.; Sokaras, D.; Steiner, J. D.; Weng, T.-C.; Nordlund, D.; Doeff, M. M.; et al. Oxygen Release Induced Chemomechanical Breakdown of Layered Cathode Materials. *Nano Lett.* **2018**, *18*, 3241−3249.
(34) Wang, Q.; Sun, J.; Chen, C. Effects of Solvents and Salt on the Thermal Stability of Lithiated Graphite Used in Lithium Ion Battery. *J. Hazard. Mater.* **2009**, *167*, 1209−1214.
(35) Nan, Y.; Li, S.; Li, B.; Yang, S. An Artificial TiO 2/Lithium n-Butoxide Hybrid SEI Layer with Facilitated Lithium-Ion Transportation Ability for Stable Lithium Anodes. *Nanoscale* **2019**, *11*, 2194−2201.
(36) Mala, K.; Jadhav, Y.; Malik, W.; Late, D.; Patil, S. I.; Jejurikar, S. Impact of MWCNT Passivation on Single Crystal Silicon Electrode: An Investigation of Electrochemical Performance and SEI Formation. *Surf. Interfaces* **2020**, *19*, No. 100476.
(37) Xu, X.; Wang, S.; Wang, H.; Hu, C.; Jin, Y.; Liu, J.; Yan, H. Recent Progresses in the Suppression Method Based on the Growth Mechanism of Lithium Dendrite. *J. Energy Chem.* **2018**, *27*, 513−527.
(38) Li, Z.; Huang, J.; Liaw, B. Y.; Metzler, V.; Zhang, J. A Review of Lithium Deposition in Lithium-Ion and Lithium Metal Secondary Batteries. *J. Power Sources* **2014**, *254*, 168−182.
(39) Parimalam, B. S.; MacIntosh, A. D.; Kadam, R.; Lucht, B. L. Decomposition Reactions of Anode Solid Electrolyte Interphase (SEI) Components with LiPF6. *J. Phys. Chem. C* **2017**, *121*, 22733−22738.
(40) Guéguen, A.; Streich, D.; He, M.; Mendez, M.; Chesneau, F. F.; Novák, P.; Berg, E. J. Decomposition of LiPF6 in High Energy Lithium-Ion Batteries Studied with Online Electrochemical Mass Spectrometry. *J. Electrochem. Soc.* **2016**, *163*, A1095.
(41) Wang, Q.; Sun, J.; Yao, X.; Chen, C. Micro Calorimeter Study on the Thermal Stability of Lithium-Ion Battery Electrolytes. *J. Loss Prev. Process Ind.* **2006**, *19*, 561−569.
(42) Kawamura, T.; Kimura, A.; Egashira, M.; Okada, S.; Yamaki, J.-I. Thermal Stability of Alkyl Carbonate Mixed-Solvent Electrolytes for Lithium Ion Cells. *J. Power Sources* **2002**, *104*, 260−264.
(43) Xu, J.; Wang, Z. C.; Yang, Y. Research Progress of the Additives to Organic Electrolytes for Secondary Li-Ion Batteries. *Chin. J. Power Sources* **2008**, *32*, 800−803.
(44) Zeng, Z.; Murugesan, V.; Han, K. S.; Jiang, X.; Cao, Y.; Xiao, L.; Ai, X.; Yang, H.; Zhang, J.-G.; Sushko, M. L.; Liu, J. Non-Flammable Electrolytes with High Salt-to-Solvent Ratios for Li-Ion and Li-Metal Batteries. *Nat. Energy* **2018**, *3*, 674−681.
(45) Hess, S.; Wohlfahrt-Mehrens, M.; Wachtler, M. Flammability of Li-Ion Battery Electrolytes: Flash Point and Self-Extinguishing Time Measurements. *J. Electrochem. Soc.* **2015**, *162*, A3084.

https://doi.org/10.1021/acs.jpcc.2c08293
J. Phys. Chem. C 2023, 127, 8195−8207

(46) Gao, T.; Wang, B.; Wang, L.; Liu, G.; Wang, F.; Luo, H.; Wang, D. LiAlCl4·3SO2 as a High Conductive, Non-Flammable and Inorganic Non-Aqueous Liquid Electrolyte for Lithium Ion Batteries. *Electrochim. Acta* **2018**, *286*, 77−85.
(47) Gu, Y.; Fang, S.; Yang, L.; Hirano, S. A Safe Electrolyte for High-Performance Lithium-Ion Batteries Containing Lithium Difluoro(Oxalato)Borate, Gamma-Butyrolactone and Non-Flammable Hydrofluoroether. *Electrochim. Acta* **2021**, *394*, No. 139120.
(48) Zeng, Z.; Jiang, X.; Wu, B.; Xiao, L.; Ai, X.; Yang, H.; Cao, Y. Bis(2,2,2-Trifluoroethyl) Methylphosphonate: An Novel Flame-Retardant Additive for Safe Lithium-Ion Battery. *Electrochim. Acta* **2014**, *129*, 300−304.
(49) Qian, Y.; Hu, S.; Zou, X.; Deng, Z.; Xu, Y.; Cao, Z.; Kang, Y.; Deng, Y.; Shi, Q.; Xu, K.; Deng, Y. How Electrolyte Additives Work in Li-Ion Batteries. *Energy Storage Mater.* **2019**, *20*, 208−215.
(50) Hastie, J. W. Molecular Basis of Flame Inhibition. *J. Res. Natl. Bur. Stand., Sect. A: Phys. Chem.* **1973**, *77A*, 733.
(51) Zhang, S. S.; Xu, K.; Jow, T. R. Enhanced Performance of Li-Ion Cell with LiBF4-PC Based Electrolyte by Addition of Small Amount of LiBOB. *J. Power Sources* **2006**, *156*, 629−633.
(52) Zhang, B.; Laszczynski, N.; Lucht, B. L. Investigation of 2, 3-Epoxypropyl Methanesulfonate (OMS) as an Electrolyte Additive for Lithium Ion Batteries. *Electrochim. Acta* **2018**, *281*, 405−409.
(53) Wu, L.; Song, Z.; Liu, L.; Guo, X.; Kong, L.; Zhan, H.; Zhou, Y.; Li, Z. A New Phosphate-Based Nonflammable Electrolyte Solvent for Li-Ion Batteries. *J. Power Sources* **2009**, *188*, 570−573.
(54) Shim, E.-G.; Nam, T.-H.; Kim, J.-G.; Kim, H.-S.; Moon, S.-I. Diphenyloctyl Phosphate as a Flame-Retardant Additive in Electrolyte for Li-Ion Batteries. *J. Power Sources* **2008**, *175*, 533−539.
(55) Baginska, M.; Sottos, N. R.; White, S. R. Core−Shell Microcapsules Containing Flame Retardant Tris(2-Chloroethyl Phosphate) for Lithium-Ion Battery Applications. *ACS Omega* **2018**, *3*, 1609−1613.
(56) Sheng, O.; Jin, C.; Luo, J.; Yuan, H.; Huang, H.; Gan, Y.; Zhang, J.; Xia, Y.; Liang, C.; Zhang, W.; Tao, X. Mg2B2O5 Nanowire Enabled Multifunctional Solid-State Electrolytes with High Ionic Conductivity, Excellent Mechanical Properties, and Flame-Retardant Performance. *Nano Lett.* **2018**, *18*, 3104−3112.
(57) Wang, Z.; Han, E.; Ke, W. Effect of Nanoparticles on the Improvement in Fire-Resistant and Anti-Ageing Properties of Flame-Retardant Coating. *Surf. Coat. Technol.* **2006**, *200*, 5706−5716.
(58) Dagger, T.; Lürenbaum, C.; Schappacher, F. M.; Winter, M. Electrochemical Performance Evaluations and Safety Investigations of Pentafluoro(Phenoxy)Cyclotriphosphazene as a Flame Retardant Electrolyte Additive for Application in Lithium Ion Battery Systems Using a Newly Designed Apparatus for Improved Self-Exting. *J. Power Sources* **2017**, *342*, 266−272.
(59) Han, L.; Liao, C.; Mu, X.; Wu, N.; Xu, Z.; Wang, J.; Song, L.; Kan, Y.; Hu, Y. Flame-Retardant ADP/PEO Solid Polymer Electrolyte for Dendrite-Free and Long-Life Lithium Battery by Generating Al, P-Rich SEI Layer. *Nano Lett.* **2021**, *21*, 4447−4453.
(60) Wang, C.; Hu, Q.; Hao, J.; Xu, X.; Ouyang, L.; Fan, W.; Ye, J.; Liu, J.; Li, J.; Mei, A.; Zhu, M. The Electrolyte Additive Effects on Commercialized Ni-Rich LiNixCoyMnzO2 (x + y + z = 1) Based Lithium-Ion Pouch Batteries at High Temperature. *ACS Appl. Energy Mater.* **2021**, *4*, 2292−2299.
(61) Li, B.; Wang, Y.; Rong, H.; Wang, Y.; Liu, J.; Xing, L.; Xu, M.; Li, W. A Novel Electrolyte with the Ability to Form a Solid Electrolyte Interface on the Anode and Cathode of a LiMn2O4/Graphite Battery. *J. Mater. Chem. A* **2013**, *1*, 12954−12961.
(62) Yeşilot, S.; Kılıç, N.; Sariyer, S.; Küçükköylü, S.; Kılıç, A.; Demir-Cakan, R. A Flame-Retardant and Insoluble Inorganic−Organic Hybrid Cathode Material Based on Polyphosphazene with Pyrene-Tetraone for Lithium Ion Batteries. *ACS Appl. Energy Mater.* **2021**, *4*, 12487−12498.
(63) Lee, H.; Han, T.; Cho, K. Y.; Ryou, M.-H.; Lee, Y. M. Dopamine as a Novel Electrolyte Additive for High-Voltage Lithium-Ion Batteries. *ACS Appl. Mater. Interfaces* **2016**, *8*, 21366−21372.
(64) Su, K.; Chen, J.; Zhang, X.; Feng, J.; Xu, Y.; Pu, Y.; Wang, C.; Ma, P.; Wang, Y.; Lang, J. Inhibition of Zinc Dendrites by Dopamine Modified Hexagonal Boron Nitride Electrolyte Additive for Zinc-Ion Batteries. *J. Power Sources* **2022**, *548*, No. 232074.
(65) Gond, R.; van Ekeren, W.; Mogensen, R.; Naylor, A. J.; Younesi, R. Non-Flammable Liquid Electrolytes for Safe Batteries. *Mater. Horiz.* **2021**, *8*, 2913−2928.
(66) Xia, L.; Xia, Y.; Liu, Z. A Novel Fluorocyclophosphazene as Bifunctional Additive for Safer Lithium-Ion Batteries. *J. Power Sources* **2015**, *278*, 190−196.
(67) Zhang, G.; Lin, X.; Zhang, Q.; Jiang, K.; Chen, W.; Han, D. Anti-Flammability, Mechanical and Thermal Properties of Bio-Based Rigid Polyurethane Foams with the Addition of Flame Retardants. *RSC Adv.* **2020**, *10*, 32156−32161.
(68) Yao, X. L.; Xie, S.; Chen, C. H.; Wang, Q. S.; Sun, J. H.; Li, Y. L.; Lu, S. X. Comparative Study of Trimethyl Phosphite and Trimethyl Phosphate as Electrolyte Additives in Lithium Ion Batteries. *J. Power Sources* **2005**, *144*, 170−175.
(69) Jiang, L.; Liang, C.; Li, H.; Wang, Q.; Sun, J. Safer Triethyl-Phosphate-Based Electrolyte Enables Nonflammable and High-Temperature Endurance for a Lithium Ion Battery. *ACS Appl. Energy Mater.* **2020**, *3*, 1719−1729.
(70) Feng, J. K.; Ai, X. P.; Cao, Y. L.; Yang, H. X. Possible Use of Non-Flammable Phosphonate Ethers as Pure Electrolyte Solvent for Lithium Batteries. *J. Power Sources* **2008**, *177*, 194−198.
(71) Nam, T.-H.; Shim, E.-G.; Kim, J.-G.; Kim, H.-S.; Moon, S.-I. Diphenyloctyl Phosphate and Tris (2, 2, 2-Trifluoroethyl) Phosphite as Flame-Retardant Additives for Li-Ion Cell Electrolytes at Elevated Temperature. *J. Power Sources* **2008**, *180*, 561−567.
(72) Nam, N. D.; Park, I. J.; Kim, J. G. Triethyl and Tributyl Phosphite as Flame-Retarding Additives in Li-Ion Batteries. *Met. Mater. Int.* **2012**, *18*, 189−196.
(73) Tsujikawa, T.; Yabuta, K.; Matsushita, T.; Matsushima, T.; Hayashi, K.; Arakawa, M. Characteristics of Lithium-Ion Battery with Non-Flammable Electrolyte. *J. Power Sources* **2009**, *189*, 429−434.
(74) Tian, X.; Yi, Y.; Fang, B.; Yang, P.; Wang, T.; Liu, P.; Qu, L.; Li, M.; Zhang, S. Design Strategies of Safe Electrolytes for Preventing Thermal Runaway in Lithium Ion Batteries. *Chem. Mater.* **2020**, *32*, 9821−9848.
(75) Chen, H.; Chen, J.; Zhang, W.; Xie, Q.; Che, Y.; Wang, H.; Xing, L.; Xu, K.; Li, W. Enhanced Cycling Stability of High-Voltage Lithium Metal Batteries with a Trifunctional Electrolyte Additive. *J. Mater. Chem. A* **2020**, *8*, 22054−22064.
(76) Chen, R.; Zhao, Y.; Li, Y.; Ye, Y.; Li, Y.; Wu, F.; Chen, S. Vinyltriethoxysilane as an Electrolyte Additive to Improve the Safety of Lithium-Ion Batteries. *J. Mater. Chem. A* **2017**, *5*, 5142−5147.
(77) Ishikawa, M.; Kawasaki, H.; Yoshimoto, N.; Morita, M. Pretreatment of Li Metal Anode with Electrolyte Additive for Enhancing Li Cycleability. *J. Power Sources* **2005**, *146*, 199−203.
(78) Fang, S.; Wang, G.; Qu, L.; Luo, D.; Yang, L.; Hirano, S. A Novel Mixture of Diethylene Glycol Diethylether and Non-Flammable Methyl-Nonafluorobutyl Ether as a Safe Electrolyte for Lithium Ion Batteries. *J. Mater. Chem. A* **2015**, *3*, 21159−21166.
(79) Ma, Y.; Yin, G.; Zuo, P.; Tan, X.; Gao, Y.; Shi, P. A Phosphorous Additive for Lithium-Ion Batteries. *Electrochem. Solid State Lett.* **2008**, *11*, A129.
(80) Jia, H.; Wang, J.; Lin, F.; Monroe, C. W.; Yang, J.; NuLi, Y. TPPi as a Flame Retardant for Rechargeable Lithium Batteries with Sulfur Composite Cathodes. *Chem. Commun.* **2014**, *50*, 7011−7013.
(81) Xu, M.; Liang, Y.; Li, B.; Xing, L.; Wang, Y.; Li, W. Tris (Pentafluorophenyl) Phosphine: A Dual Functionality Additive for Flame-Retarding and Sacrificial Oxidation on LiMn2O4 for Lithium Ion Battery. *Mater. Chem. Phys.* **2014**, *143*, 1048−1054.
(82) Zhu, X.; Jiang, X.; Ai, X.; Yang, H.; Cao, Y. Bis (2, 2, 2-Trifluoroethyl) Ethylphosphonate as Novel High-Efficient Flame Retardant Additive for Safer Lithium-Ion Battery. *Electrochim. Acta* **2015**, *165*, 67−71.
(83) Maheshwaran, C.; Kanchan, D. K.; Mishra, K.; Kumar, D.; Gohel, K. Effect of Active MgO Nano-Particles Dispersion in Small

https://doi.org/10.1021/acs.jpcc.2c08293
J. Phys. Chem. C 2023, 127, 8195−8207

Amount within Magnesium-Ion Conducting Polymer Electrolyte Matrix. *Nano-Struct. Nano-Objects* **2020**, *24*, No. 100587.
(84) Xu, M.; Lu, D.; Garsuch, A.; Lucht, B. L. Improved Performance of LiNi0. 5Mn1. 5O4 Cathodes with Electrolytes Containing Dimethylmethylphosphonate (DMMP). *J. Electrochem. Soc.* **2012**, *159*, A2130.
(85) Darve, E.; Pohorille, A. Calculating Free Energies Using Average Force. *J. Chem. Phys.* **2001**, *115*, 9169−9183.
(86) Bhatnagar, N.; Kamath, G.; Chelst, I.; Potoff, J. J. Direct Calculation of 1-Octanol−Water Partition Coefficients from Adaptive Biasing Force Molecular Dynamics Simulations. *J. Chem. Phys.* **2012**, *137*, 014502.
(87) Kamath, G.; Baker, G. A. In Silico Free Energy Predictions for Ionic Liquid-Assisted Exfoliation of a Graphene Bilayer into Individual Graphene Nanosheets. *Phys. Chem. Chem. Phys.* **2012**, *14*, 7929−7933.
(88) Shakourian-Fard, M.; Kamath, G.; Sankaranarayanan, S. K. R. S. Evaluating the Free Energies of Solvation and Electronic Structures of Lithium-Ion Battery Electrolytes. *ChemPhysChem* **2016**, *17*, 2916−2930.
(89) Kamath, G.; Cutler, R. W.; Deshmukh, S. A.; Shakourian-Fard, M.; Parrish, R.; Huether, J.; Butt, D. P.; Xiong, H.; Sankaranarayanan, S. K. R. S. In Silico Based Rank-Order Determination and Experiments on Nonaqueous Electrolytes for Sodium Ion Battery Applications. *J. Phys. Chem. C* **2014**, *118*, 13406−13416.
(90) Shakourian-Fard, M.; Kamath, G.; Sankaranarayanan, S. K. R. S. Electronic Structure Insights into the Solvation of Magnesium Ions with Cyclic and Acyclic Carbonates. *ChemPhysChem* **2015**, *16*, 3607−3617.
(91) Phillips, J. C.; Braun, R.; Wang, W.; Gumbart, J.; Tajkhorshid, E.; Villa, E.; Chipot, C.; Skeel, R. D.; Kale, L.; Schulten, K. Scalable Molecular Dynamics with NAMD. *J. Comput. Chem.* **2005**, *26*, 1781−1802.
(92) Vanommeslaeghe, K.; Hatcher, E.; Acharya, C.; Kundu, S.; Zhong, S.; Shim, J.; Darian, E.; Guvench, O.; Lopes, P.; Vorobyov, I. CHARMM General Force Field: A Force Field for Drug-like Molecules Compatible with the CHARMM All-atom Additive Biological Force Fields. *J. Comput. Chem.* **2010**, *31*, 671−690.

https://doi.org/10.1021/acs.jpcc.2c08293
J. Phys. Chem. C 2023, 127, 8195−8207